

Synchronization of electronic genetic networks

Alexandre Wagemakers,¹ Javier M. Buldú,² Jordi García-Ojalvo,² and Miguel A.F. Sanjuán¹

¹ *Nonlinear Dynamics and Chaos Group*

*Departamento de Matemáticas y Física Aplicadas y Ciencias de la Naturaleza,
Universidad Rey Juan Carlos, Tulipán s/n, 28933 Móstoles, Madrid, Spain.*

² *Departament de Física i Enginyeria Nuclear,
Universitat Politècnica de Catalunya, Colom 11, 08222 Terrassa, Spain.*

(Dated: January 17, 2006)

Abstract

We describe a simple analog electronic circuit that mimics the behavior of a well-known synthetic gene oscillator, the repressilator, which represents a set of three genes repressing one another. Synchronization of a population of such units is thoroughly studied, with the aim to comparing the role of global coupling with that of global forcing on the population. Our results show that coupling is much more efficient than forcing in leading the gene population to synchronized oscillations. Furthermore a modification of the proposed analog circuit leads to a simple electronic version of a genetic toggle switch, which is a simple network of two mutually repressor genes, where control by external forcing is also analyzed.

PACS numbers: 87.16.Ac, 87.14.Ee, 87.19.Jj

One of the main advances brought about by the advent of synthetic biology is the design of artificial gene regulation networks that mimic the behavior of natural ones. One could think that this simplifies the analysis of cell behavior by isolating in a modular way relevant network modules, which can therefore be studied independently of other complex cellular processes that in the natural case are intermingled with the module of interest. This is certainly the case, and has been the main motivation behind the design of certain synthetic gene networks, such as oscillators and switches. A paradigmatic example is the repressilator, a set of three genes (and their respective proteins) which repress one another in a circular way, leading to clear-cut oscillations in protein expression. In spite of their doubtless advantages, experimental studies of these synthetic systems are still difficult, due both to the inherent complexity of molecular biology experiments and to our lack of knowledge of the kinetic parameters of the specific network components. For example, mutual synchronization of globally coupled populations of repressilators has not yet been observed, in spite of theoretical predictions and of the interest of the phenomenon as a model of synchronized rhythm generation in multicellular circadian clocks. Here we take another approach, reproducing the dynamical behavior of the repressilator via a simple analog electronic circuit, and using it to investigate experimentally the synchronization of a set of repressilators, with an emphasis on the comparison between the effect of global coupling and global external forcing, two ingredients that can realistically be expected to exist in natural multicellular clocks. The usefulness of the approach is further demonstrated by the design of an even simpler circuit representing a genetic toggle switch, and its use to study the effect of forcing on a population of such devices.

I. INTRODUCTION

Genetic regulatory networks have been well studied in living microorganisms such as bacteria or viruses since the early 1960s [1]. They rely on the fact that certain specific proteins are able to influence and regulate the activity of DNA transcription. The final product of this DNA transcription is another protein, which could influence in turn the

expression of yet another gene (or of its own gene, or even that of its transcription factor). This process leads to networks of genetic interactions, where proteins and genes can be interpreted as nodes, and the interactions between them as links [2]. These regulatory networks provide the essential control of protein expression in the cell.

Transcription regulation can arise in a positive or negative way. Negative regulation occurs when a protein hinders, or even blocks, the transcription process. For instance when a protein binds at a certain location of the DNA chain, called *promoter*, it blocks the access of RNA polymerase, which is the enzyme that transcribes DNA into messenger RNA. This kind of proteins are called *repressors*. An example of repressive regulation is the tryptophan *trp* operon in the bacterium *Escherichia coli* (*E. coli*), where the presence of tryptophan proteins inhibits the transcription of the *trp* operon [3]. On the other hand, positive regulation results from biochemical processes that enhance protein transcription, or at least allow it. The regulation of the lactose operon in *E. coli* is a good example of positive regulation [1]. The presence of β -galactosidase in the bacteria's medium speeds up the transcription of the operon, and consequently the bacteria can transform lactose in glucose.

These mechanisms of positive and negative regulation are similar to control mechanisms in electrical engineering. Negative feedback regulation is a basic system of control that enhances the stability and the resistance to noise in gene expression [4].

Gene regulation is the basis of the design of synthetic regulatory pathways. In our context, synthetic means that the genetic network does not exist in a natural form. The first synthetic genetic networks, a genetic toggle switch [5] and a genetic oscillator [6], have been presented in two seminal articles. In Ref. [5], the combination of two mutually repressing genes forms a bistable system whose state can be changed due to an external inducer (e.g. a protein or a temperature shift). When one of the transcribed proteins is produced, the other one remains silenced. The switching occurs when the inducer (external influence) is applied beyond a certain threshold, making the system jump to the opposite state. After a jump between states, which consists in a variation of the protein concentration, the system maintains the protein level. One can say that this genetic switch has memory, since it remains in its current state until an external inducer acts again.

The second paradigmatic system is the repressilator [6], which is in fact a genetic oscillator and where three repressor genes are placed in a ring, with each repressor inhibiting the

production of the following protein with a certain delay. In Fig. 1(a) we show a schematic representation of the interactions of this genetic network, where blue arrows represent promoters. The product of each repressor gene (in green) binds to the next promoter and inhibits production of the corresponding protein. This configuration leads to oscillations in the expression of the three proteins, with a $2\pi/3$ phase delay. Driven by this network motif, different bacteria oscillate independently, with different phases and slightly different frequencies (due to intrinsic cell variability) [6]. Synchronization of these rhythms would allow global oscillations in the cell population, thus simplifying the observation of the phenomenon, which currently requires single-cell tracking. Intercell communication through quorum-sensing has been proposed as a mechanism of synchronization [7], but no experimental verification has been made so far.

In this paper, we propose an analysis of the dynamics of these two genetic regulatory networks (repressilator and toggle switch), making use of nonlinear analog electronic circuits. Our circuits allow a one-to-one correspondence between the structure of the genetic and electronic networks, and their analog character extends this correspondence to the full dynamical behavior. An evident benefit is that the electronic circuits are easier to implement experimentally than genetic circuits. The natural parameter mismatch in the living cell is reproduced by component dispersion in the electronic circuits. We study the synchronization of a population of repressilators due to global coupling. Additionally, in order to improve the synchronization of the genetic oscillators we add an external periodical forcing to every repressilator. We analyse the influence of external forcing on synchronization when the frequency and the amplitude of the external signal are modified. The results obtained with electronic circuits should be extensible to synthetic genetic networks, where external forcing could be implemented via a temperature periodic shift, or by periodic injection of a repressor protein. Finally, we develop an electronic toggle switch by mutually coupling two MOS transistors, and reproduce the dynamics of the corresponding synthetic genetic network. In particular, we study the response of a population of toggle switches to global external forcing. The organization of the paper is as follows. In Sec. II, we introduce the electronic repressilator. In Sec. III, the coupling of the population of repressilators is carried out, while in Sec. IV a global periodical forcing is applied. The electronic toggle switch is described in Sec. V. And finally in Sec. VI we summarize our results.

II. THE ELECTRONIC REPRESSILATOR

Previous work on electronic genetic networks used hybrid digital-analog circuits based on AND and OR functions [8]. Here we propose the use of all-analog circuits whose structure and dynamics are as similar as possible to that of the corresponding genetic network. Fig. 1(b) shows the electronic setup of the analog repressilator. The output of the three MOS transistors correspond to the level of the three repressor proteins of the repressilator. The numerical values of the resistances, and capacitances are indicated in Table I. Two reasons have motivated this particular design. First, the simplicity of the circuit, which is composed of basic electronic components. Second, the fact that the MOS technology allows the use of the analog repressilator in integrated circuits.

The N-channel MOSFET transistors of Fig. 1(b) can be viewed as controllable switches. If the tension applied to the gate exceeds a certain threshold voltage, the transistor switches

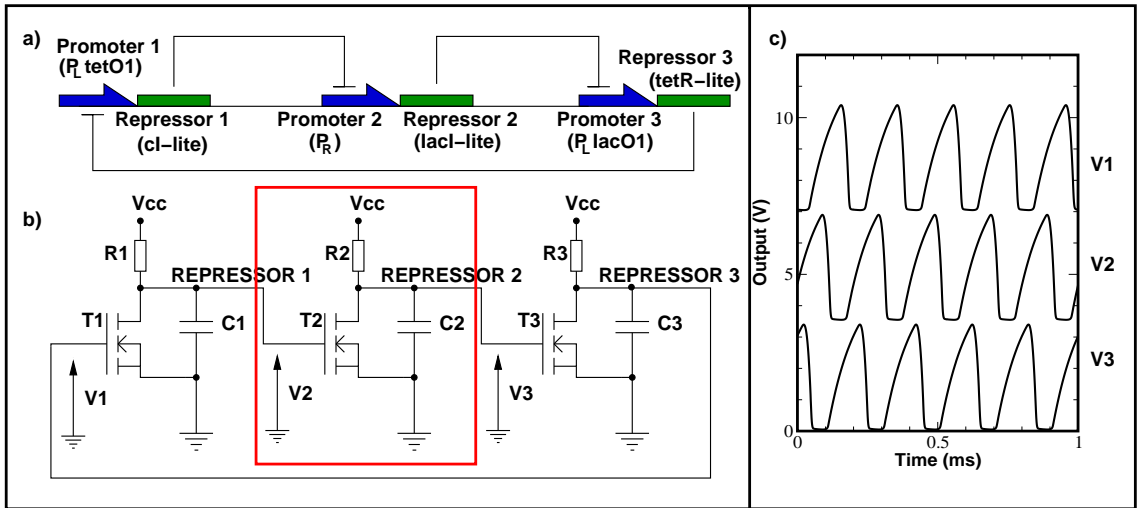


FIG. 1: a) Network architecture of a synthetic oscillator, the repressilator. Three repressor genes are consecutively connected by negative feedback. Promoters (in blue) of each gene (in green) are repressed by proteins (cI, LacI and TetR) transcribed from the previous gene. b) Electronic setup of the analog repressilator. Only three kind of elements are required: resistances, MOS transistors and capacitances. The output of each transistor corresponds to the level of each repressor protein. c) Dynamics of the electronic repressilator. Time series (displaced in the vertical axes to allow comparison) of the three analog protein concentrations. They oscillate at the same frequency but phase shifted by $2\pi/3$.

Symbol	Parameter	Values	Units
R_i	Internal resistance	$1.0 \pm 10\%$	$k\Omega$
C_i	Internal capacitance	$1.0 \pm 20\%$	μF
T_i	Transistor 2N7000	–	–
V_1	Voltage source	3.227	V
R_i^c	Coupling resistance	from 0.130 to 30	$k\Omega$

TABLE I: Numerical values of the electronic components used in the experiment

off its output, leading to an output voltage close to zero (the transistor has very low output impedance). In this case, the tension on the gate acts as a repressor of the output voltage, similar to what happens with a repressor protein. When the gate voltage V_2 falls below the threshold, the voltage V_3 associated to transistor T2 begins to increase and the transistor T2 acts as a high-level impedance, that is, we have an open circuit. The protein level is represented by the output voltage of the transistors (and capacitors). In the absence of repression (no tension on V_2), the transistor voltage V_3 , which in turn will be the repressor of the following transistor, grows until it reaches its maximum value (the supply voltage V_{cc}). On the other hand, if repression rises, due to an increase of voltage at the previous transistor, the output voltage falls to zero. Summarizing, we can say that the three transistors are repressing themselves in the same way as it happens in the repressilator genetic network. This kind of configuration is responsible of the oscillations at the three output voltages/protein levels and is known as a *ring oscillator*.

We can derive the differential equations of this model by considering a basic unit (equivalent to a single repressor gene), which is made of a RC circuit connected to a voltage source and a transistor [see red square at Fig. 2(b)]. Without any voltage V_2 on the gate of the transistor T2, it will behave as a simple RC circuit. The transistor will be turned off and the capacitor will be charged until it reaches its maximum value. If the gate voltage increases and reaches a certain threshold V_{th} , the transistor T2 “cuts” the output tension and the capacitor discharges rapidly through the transistor. From this simple circuit we can derive the differential equation of the variable V_3

$$R_2 C_2 \frac{dV_3}{dt} = -V_3 + V_{cc} f(V_2), \quad (1)$$

where the function $f(x)$ depends on the transistor parameters and should be sigmoidal

shaped if we want to obtain oscillations at the transistor's output. A good candidate for $f(x)$ is

$$f(x) = \frac{\alpha}{1 + \beta x^n}, \quad (2)$$

where α , β and n are parameters depending on the MOSFET transistor. This corresponds to the Michaelis-Menten equation of growth of order n .

The complete set of equations of the repressilator reads

$$R_1 C_1 \frac{dV_2}{dt} = -V_2 + V_{cc} f(V_1) \quad (3)$$

$$R_2 C_2 \frac{dV_3}{dt} = -V_3 + V_{cc} f(V_2) \quad (4)$$

$$R_3 C_3 \frac{dV_1}{dt} = -V_1 + V_{cc} f(V_3). \quad (5)$$

And the time series of the circuit can be seen in Fig. 1(c), where the three repressor levels evolve with a phase difference of $2\pi/3$. When a repressor is active (e.g. T1 voltage), the following repressor (T2) is inhibited and the third increases (T3). The increase of T3 leads, in turn, to the decrease of T1 voltage. The chain repression is responsible of the oscillations of the whole system, both in electronic and genetic repressilators.

III. COUPLING ELECTRONIC REPRESSILATORS

One of the questions raised by the seminal paper of Elowitz *et al.* [6] is the way that a population of repressilators might be synchronized. It has been observed that each cell of a colony of repressilators oscillates at its own frequency and phase, preventing the occurrence of global oscillations. Intercell communication via quorum sensing [9, 10] has been proposed as a way of coupling repressilators [7], with the aim of observing global oscillations of the colony. In this section, we reproduce the numerical observations of [7] using a collection of globally coupled electronic repressilators. The internal parameters of the circuits are adjusted to make them oscillate at different frequencies, and a global coupling is introduced through a resistance R_i^c placed at the output of the first transistor (T1) of each repressilator. All coupling resistances are connected to a common point, allowing an exchange of information about the dynamical state of the repressilators through the intensities of each branch. The coupling intensity is controlled by adjusting the values of R_i^c , which are set to be the same: coupling increases as the coupling resistance decreases. The experimental setup is composed

of 16 coupled electronic repressilator. One of the dynamical variable of the 16 circuits is recorded with a A/D converter board with 16 inputs.

Figure 2(d,e,f) shows the temporal evolution of a population of 16 electronic repressilators for increasing coupling (that is decreasing coupling resistance R^c). Time series correspond to the voltage at the output of the first transistor. Panels (a,b,c) of the figure show the probability distribution function (pdf) of the period between oscillations. For low coupling ($R_i^c = 5.1 \text{ k}\Omega$), repressilators oscillate unsynchronized at their own frequency (upper plots), and the pdf has a wide distribution of periods. Intermediate values of coupling ($R_i^c = 2.2 \text{ k}\Omega$), show a partial entrainment (central plots), which is reflected by the appearance of a peak at the pdf. Finally, when coupling is further increased ($R_i^c = 0.24 \text{ k}\Omega$), we achieve synchronization of all repressilators (bottom plots), denoted by the unique peak at the pdf.

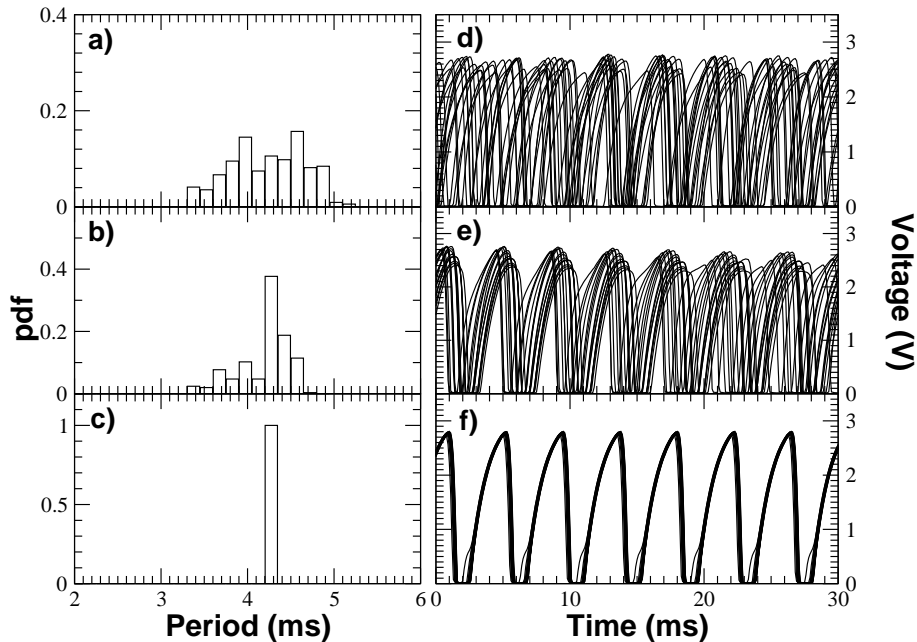


FIG. 2: Experimental time series (d,e,f) and probability distribution function (pdf) of the oscillation periods (a,b,c) for a population of 16 repressilators. The coupling strength increases when the resistance decreases (the currents between the coupled circuits flow easier). In this figure we show three cases starting from low coupling (upper figures) to high coupling (lower figures). From upper figure to lower figure we have: low $R_i^c = 5.1 \text{ k}\Omega$ (a,d), intermediate $R_i^c = 2.2 \text{ k}\Omega$ (b,e) and high $R_i^c = 0.24 \text{ k}\Omega$ coupling (c,f). Note that the coupling is measured by the inverse of R_i^c in such a way that when R_i^c decreases the coupling increases.

It is worth noting that repressilators oscillate not only at the same frequency but also at the same phase, a fact that can only be observed at the time series of the voltage as shown in Fig. 2.e. Our experimental observations agree qualitatively with the numerical simulations of [7] and confirm that global coupling would be a suitable way of obtaining synchronization of a colony of repressilators.

Figure 3 shows a systematic study of the influence of coupling in the synchronization of the population of repressilators. We have evaluated the order parameter R given by the expression

$$R = \frac{\langle \overline{V_{2,i}^2} \rangle - \langle \overline{V_{2,i}} \rangle^2}{\langle V_{2,i}^2 \rangle - \langle V_{2,i} \rangle^2}, \quad (6)$$

where $V_{2,i}(t)$ corresponds to the voltage at the T1 output of repressilator i , $\langle \dots \rangle$ indicates time average and $\overline{\dots}$ denotes average over the population of repressilators. Low values of R correspond to the absence of coherent fluctuations of the system, while R close to the unity indicates a high coherence of the oscillations. Figure 3 corresponds to the classic synchronization phase transition predicted by Kuramoto [11] in coupled phase oscillators [12], and has been reported experimentally in coupled electrochemical oscillators [13] and in numerical simulations of a population of repressilators [7].

IV. FORCING ELECTRONIC REPRESSILATORS

Synchronization of a population of repressilators by global coupling, reported above for our analog electronic circuits, has not yet been reproduced in a real biochemical setting. In this paper we propose a parallel source of entrainment, which can be provided by external influences [14]. An extra motivation in our case arises from the behavior of circadian rhythms, biochemical rhythms with a period close to 24 hours that have been observed ubiquitously among living organisms [15]. In the absence of external cues, the internal rhythms of such organisms drift with periods close to (but different from) 24 hours, but in the presence of external forcing they become perfectly entrained to the external period. In many organisms, the source of external forcing has been identified to be a variation of the light due to night and day cycles. Indeed, the molecular basis of the effect of light on different circadian biochemical networks has been unraveled [16]. The question on whether such external forcing is enough to induce the synchronization between circadian cells usually observed in exper-

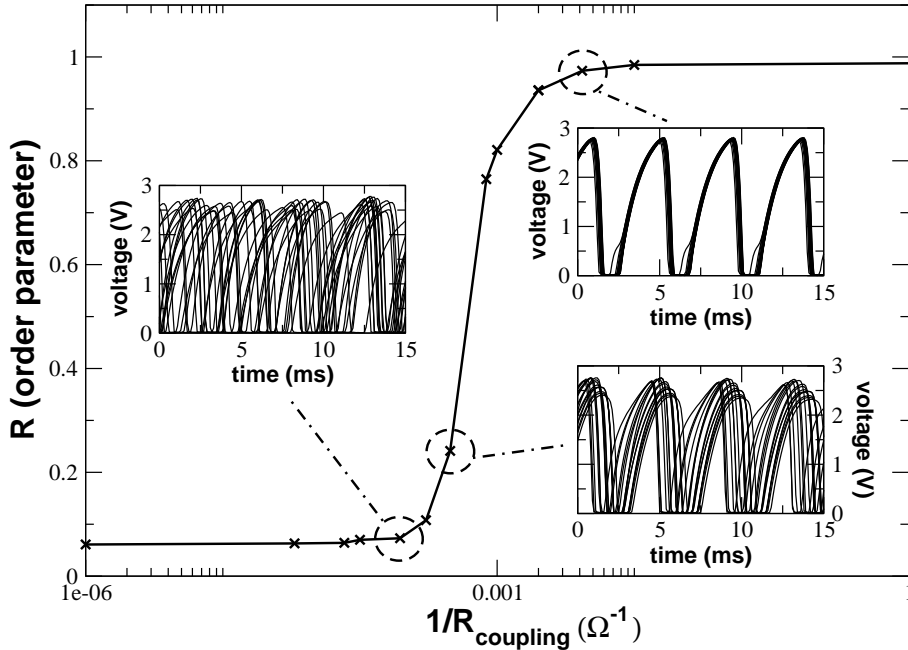


FIG. 3: Synchronization transition of a population of electronic repressilators for increasing values of the coupling parameter. An order parameter R (see Eq. (6)) close to one indicates synchronization of the population of repressilators for values of $1/R_i^c > 0.001\Omega^{-1}$. This figure shows the characteristic transition to synchrony of a population of coupled oscillators when the coupling is increased.

iments [17], or if coupling between the cells is needed, is still open. This is precisely what we address here, with the help of electronic circuits.

We consider a population of electronic repressilators oscillating within a certain range of frequencies, i.e., in the absence of global oscillations. When a periodic external forcing is applied to the whole population, all repressilators would be affected by the same external frequency, leading to global oscillations. In our case, the electronic repressilators are forced by modulating the common point of the coupling resistances (see Fig. 4). An intermediate coupling resistance $R_f = 0.24 \text{ k}\Omega$ is placed between the common point and an external forcing voltage. The intensity of the forcing is controlled by the amplitude of the external voltage.

This configuration allows to adjust both the coupling and the forcing of the system and analyze its combined effect on the synchronization of a population of repressilators. Figure 5 plots the time series (insets) and the power spectra of the whole system (16 repressilators)

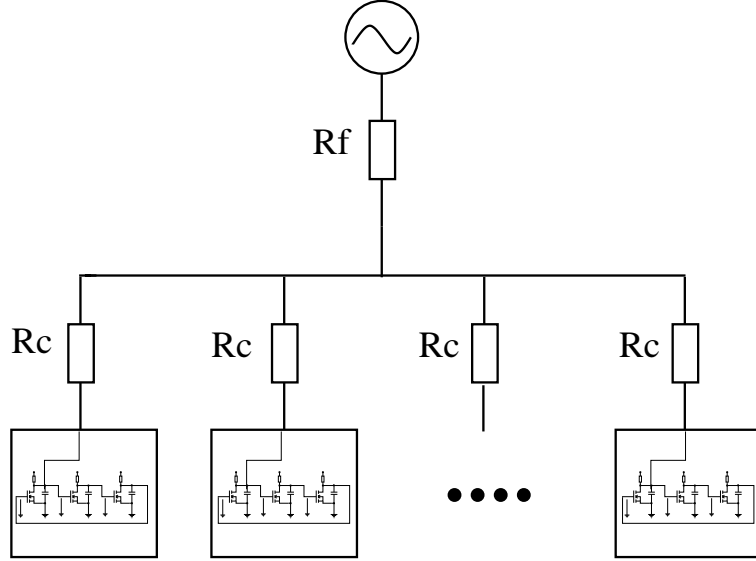


FIG. 4: Schematic representation of a population of globally coupled electronic repressilators. The coupling among the repressilators is controlled with the resistance R_c . A function generator forces all units in the same way. The amplitude of the forcing can be controlled via the output voltage of the generator or through the resistance R_f .

for three different forcing amplitudes A_f , and a given forcing frequency $f_f = 240$ Hz. We have chosen the forcing frequency to be within the frequency range of the unsynchronized repressilators (150 Hz. . . 300 Hz). In order to study only the influence of forcing, the coupling resistance is set to $R_c^c = 5.1$ k Ω , which corresponds to a negligible coupling [see Fig. 2(a)]. For low values of forcing $A_f = 1$ V [Fig. 5(a)], repressilators keep their oscillating frequencies, as shown by the time series and the wide power spectrum. If the forcing amplitude is increased $A_f = 2.4$ V, we observe a reduction of the spectrum amplitude and an appearance of a central peak at the forcing frequency $f_f = 240$ Hz [Fig. 5(b)]. At the same time, some repressilators seem to be frequency locked (inset of Fig. 5(b)). Finally, for high enough values of the forcing amplitude, $A_f = 4$ V, the power spectrum shows a unique peak, indicating that oscillators are frequency locked [Fig. 5(c)]. Nevertheless, a phase shift is kept between them, as can be observed at the temporal evolution of their output voltages (inset of Fig. 5(c)).

Now we consider different forcing frequencies, since it is well known that nonlinear oscillators can adjust their period of oscillations within a certain range of frequencies [18]. In

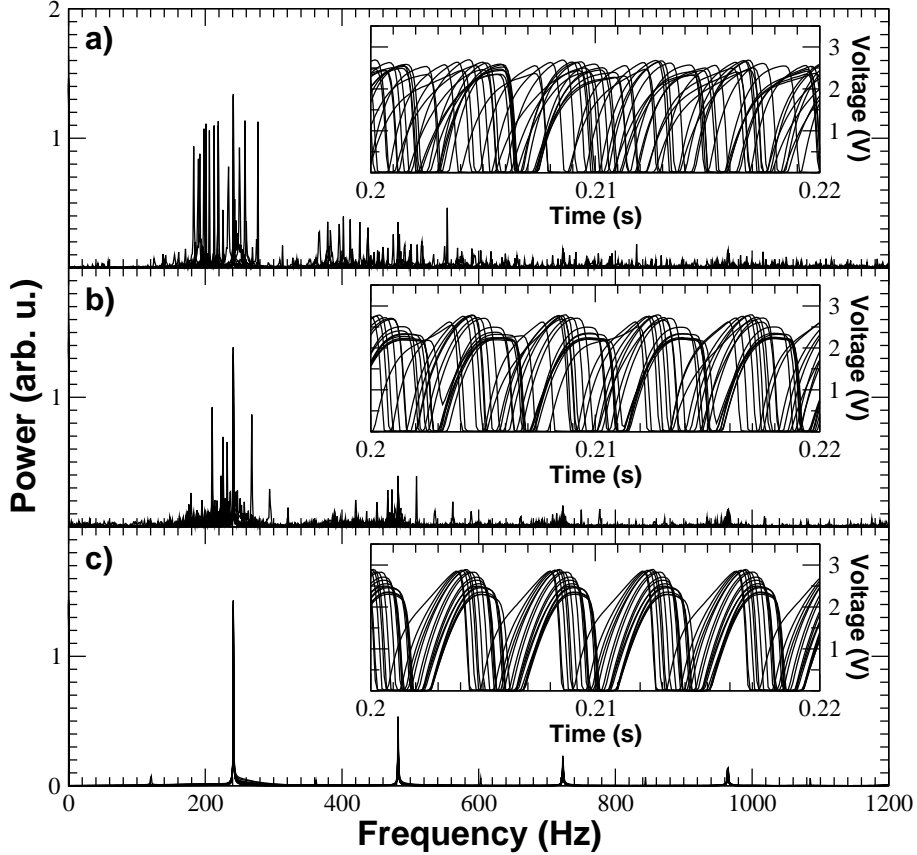


FIG. 5: Transition to synchronization by an external forcing of frequency $f_f = 240$ Hz: power spectrum of 16 repressilators for varying values of external forcing and their corresponding time series (inset). The coupling between the units is set to a low value, so that we focus on the influence of forcing. The three figures show the power spectrum for increasing values of the forcing: (a) weak forcing $A_f = 1V$; (b) intermediate forcing $A_f = 2.4V$; (c) strong forcing $A_f = 4V$. For a weak forcing each unit present a different frequency of oscillation. At intermediate coupling some of the repressilators locked their frequency. At strong coupling values the system is synchronized.

Fig. 6 we plot the power spectrum and the corresponding time series for three different forcing frequencies f_f and a given forcing amplitude $A_f = 4$ V. We have chosen the forcing frequencies to be inside (b) and outside (a,c) the frequency distribution range of the population of repressilators. When the forcing frequency is too low, repressilators do not follow it, and the power spectrum does not show any peak at the forcing frequency [Fig. 6(a)]. If the forcing frequency enters a region close to the natural frequencies of the repressilators, the system is entrained by the forcing frequency [Fig. 6(b)]. Nevertheless we still observe a phase shift at the time series (inset). The entrainment is optimum for a central frequency

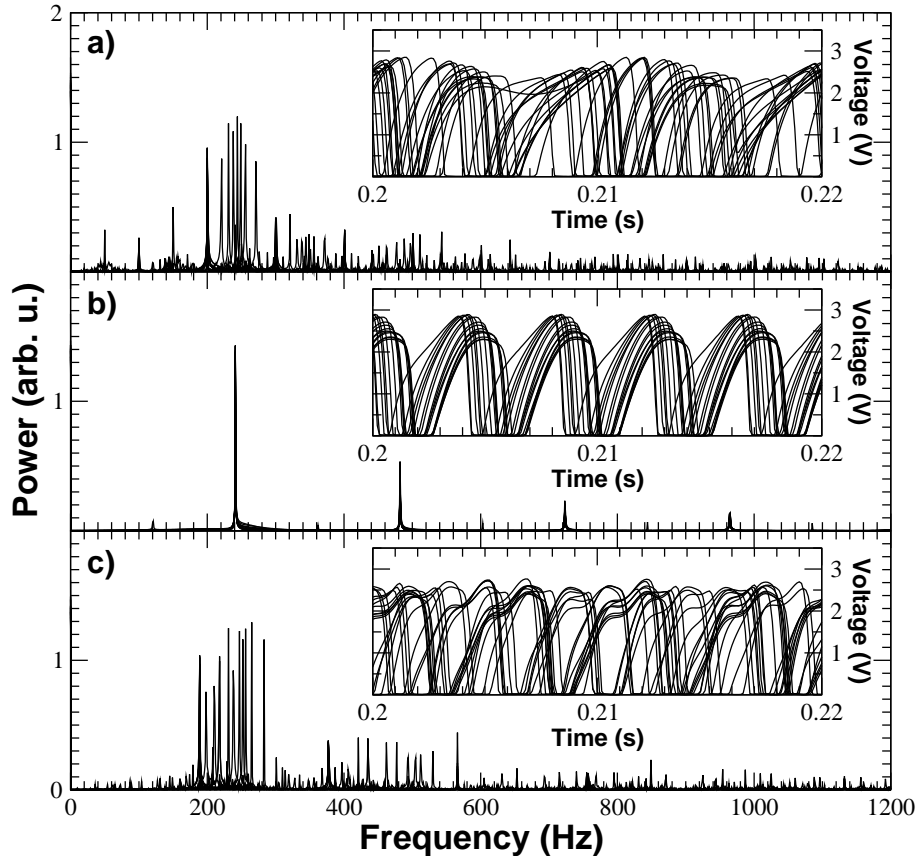


FIG. 6: Influence of the external frequency on the synchronization of analog repressilators. We fix the amplitude of the external forcing to a high enough value $A_f = 4V$ while its frequency f_f is modified in a range close to the natural frequency of the repressilator population. In a) although the forcing strength is high, synchronization is not observed for low values of the forcing frequency $f_f = 100$ Hz. In b) the entrainment is achieved when the forcing frequency $f_f = 240$ Hz is close to the natural frequency of the electronic repressilators. In c) we lose again synchronization if the forcing frequency is further increased, $f_f = 560$ Hz.

$f_f = 240$ Hz and it is gradually lost when the frequency is further increased [Fig. 6(c)].

At this point it is worth noting the differences between forcing and coupling. Figure 7 shows the synchronization of the population of repressilators for the two different techniques. We can see that despite of having the same power spectrum, i.e., the same oscillating frequency, the time series show a phase shift between repressilators only for the case of forcing. In fact, we must distinguish between two different synchronized states. In the case of a coupled population, we achieve both frequency and phase locking leading to an order parameter

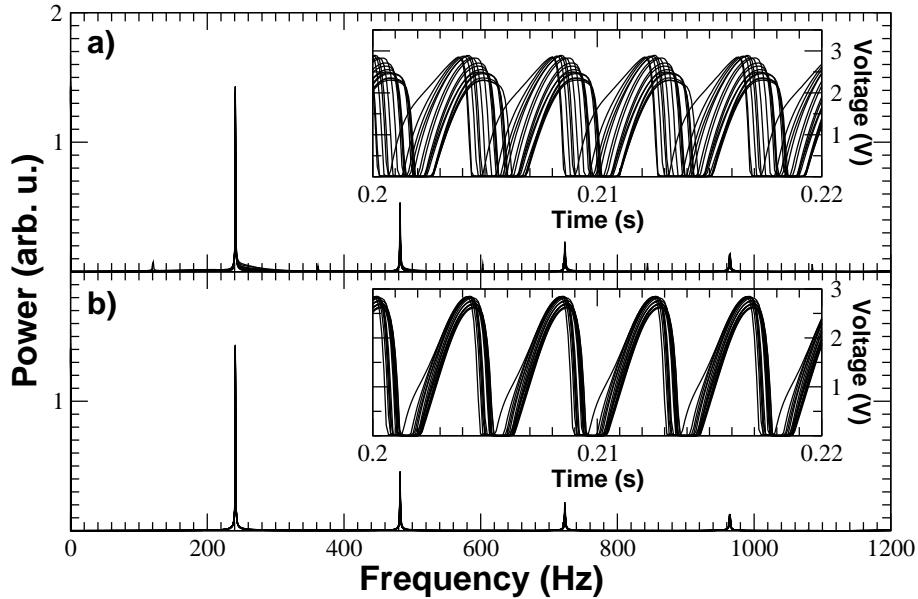


FIG. 7: Comparison between synchronization by forcing (a) and coupling (b). We can observe that although both spectra are similar, which means that there is an entrainment to the external frequency, the phase difference only disappears when repressilators are coupled (b). The population of repressilators oscillates at the forcing frequency nevertheless when the coupling between units disappears a phase deviation appears between the units.

R close to the unity. Nevertheless, when we introduce external forcing in an uncoupled system, we observe only frequency locking and the phases of each oscillator depend on its initial conditions. This fact slightly reduces the efficiency of this technique, decreasing the amplitude of the global oscillations.

If coupling and forcing are considered at the same time, a better entrainment of the global oscillations would be expected. To check this conjecture we scan the amplitude and frequency of the forcing signal in the absence or presence of coupling. In Fig. 8 we plot the results obtained with a frequency step of $\Delta f = 20$ Hz and an amplitude step of $\Delta A = 0.5$ V. Two cases are shown; the left plot corresponds to negligible coupling between repressilators, whereas coupling and forcing are jointly considered in the right plot. For the latter case, we set the coupling to intermediate values [$R_i^c = 2.2$ k Ω , see Fig. 2(b)].

At first sight, a resonance region appears in both cases, although some differences exist. In the absence of coupling (left plot), the synchronization region is reduced, showing a sharp peak. In addition, we observe low peaks at the first harmonic of the resonance frequency.

Nevertheless the highest value corresponds to $R = 0.46$, which is considerably low compared with the highest peak of the coupling case $R = 0.92$. Such differences are caused by the phase shift, since the order parameter R measures correlations between series at zero lag (i.e. without phase shift). If coupling is considered (right plot), R has high values even for the case of forcing at low/high frequencies. Synchronization is increased when the forcing frequency enters the region of natural frequencies of the system. Furthermore, resonances at the first harmonic of the natural frequencies are also observed.

These results indicate that external forcing enhances synchronization in a population of globally coupled repressilators. However, these results are not so good when the coupling is suppressed or reduced to a negligible part. With only the forcing acting, a phase shift between the repressilators appears as in the inset of Fig. 5(c) and the total coherence R of the system decreases.

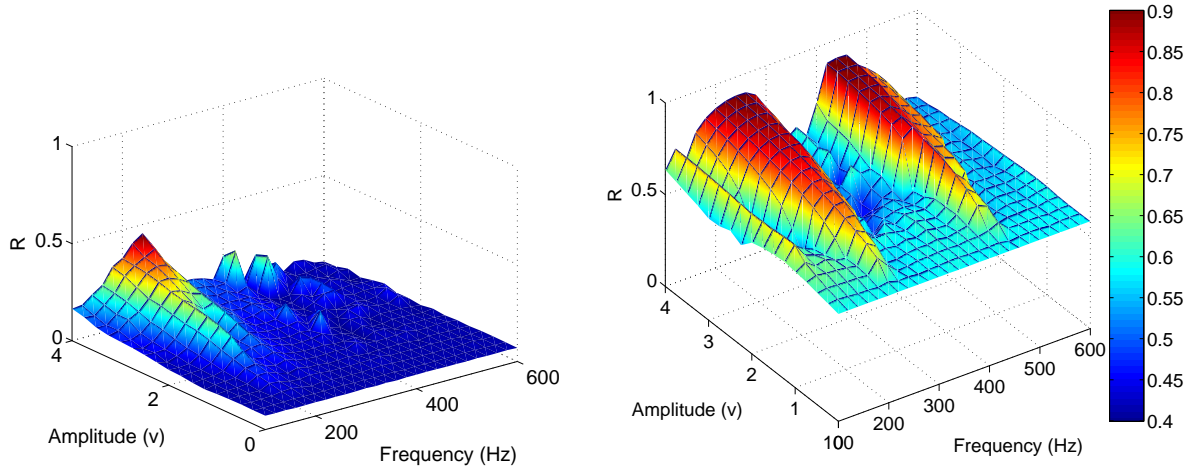


FIG. 8: Synchronization efficiency of external forcing in the presence (right plot) and absence (left plot) of coupling. The axes correspond to the forcing frequency (X), forcing amplitude (Y) and the corresponding order parameter (Z). In the absence of coupling (left plot), we observe a maximum (resonance) close to the region of the natural frequency of the repressilators. We can also observe a low peak close to the first harmonic of the resonance frequency. When coupling and forcing are considered, we can observe an increase of the order parameter. Nevertheless we can still observe a region where the system enters resonance with the external forcing. The peak at the first harmonic has increased (compared with the uncoupled case) and both resonance regions are now wider.

V. THE ELECTRONIC TOGGLE SWITCH

Following the same procedure as in the electronic repressilator, we can build other electronic-circuit representation of genetic networks. For example, removing one transistor from the repressilator circuit leads to a bistable system similar to the toggle switch developed in [5] by Gardner *et al.* The toggle switch is a simple network of two repressor genes, where each of the repressor proteins binds to the promoter of the other one [see Fig. 9(a)]. In this way, when a repressor dominates, the system remains at the same state unless an external effect changes it, by degrading artificially one of the repressors, so the other one takes over and the state is changed.

The design of the circuit is similar to the electronic repressilators, but it contains only two basic units, each one consisting of a transistor and a RC circuit. We assume that the

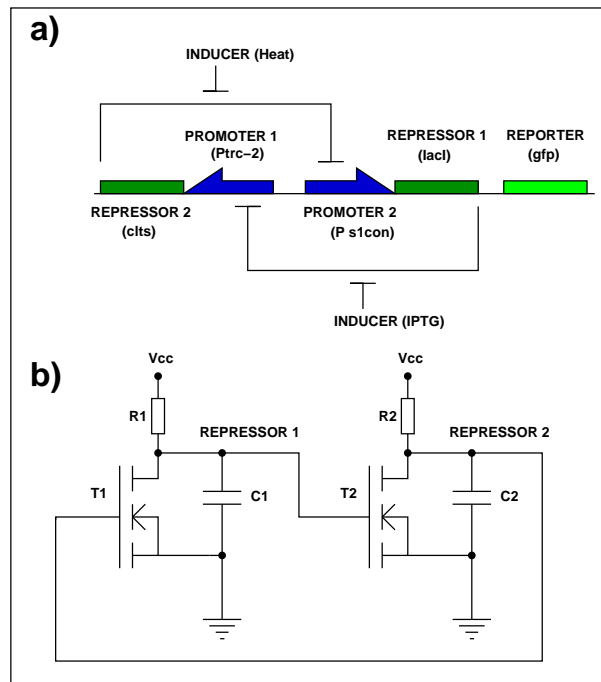


FIG. 9: a) Network architecture of a bistable genetic network toggle-switch. Two repressor genes are mutually connected by negative feedback. Promoters (in blue) of each gene (in green) are repressed by proteins transcribed from the previous gene. A green fluorescent protein (GFP), associated to a protein (cI) level, acts as the reporter of the system state. b) Electronic setup of the analog toggle-switch. The output of each transistor corresponds to the level of the two repressor proteins.

voltage of one component (T1) is large. Since it is applied at the gate of the other transistor (T2), it inhibits the second component, whose output voltage is switched off. The differential equations of the system are:

$$R_1 C_1 \frac{dV_1}{dt} = -V_1 + V_{cc}(1 - f(V_2)) \quad (7)$$

$$R_2 C_2 \frac{dV_2}{dt} = -V_2 + V_{cc}(1 - f(V_1)) \quad (8)$$

where the function $f(x)$ was given in Eq. 2. The phase portrait of the system, **which is displayed in Fig. 10**, contains three **stationary points**, two of them stable and the other one unstable. Moreover it is divided into two parts with a separatrix marking the boundary between the two basins of attraction. When the state of the system crosses the separatrix after being forced, it jumps to the other basin of attraction and a switching occurs.

First of all, we must check the switching properties of the Electronic Toggle Switch (ETS). In bistable systems, switching between states must be produced by external induction. In our case, the inducer is an external voltage source, whose potential is applied through a discharge resistance R_d . Since the system is bistable, we first turn off the output voltage of

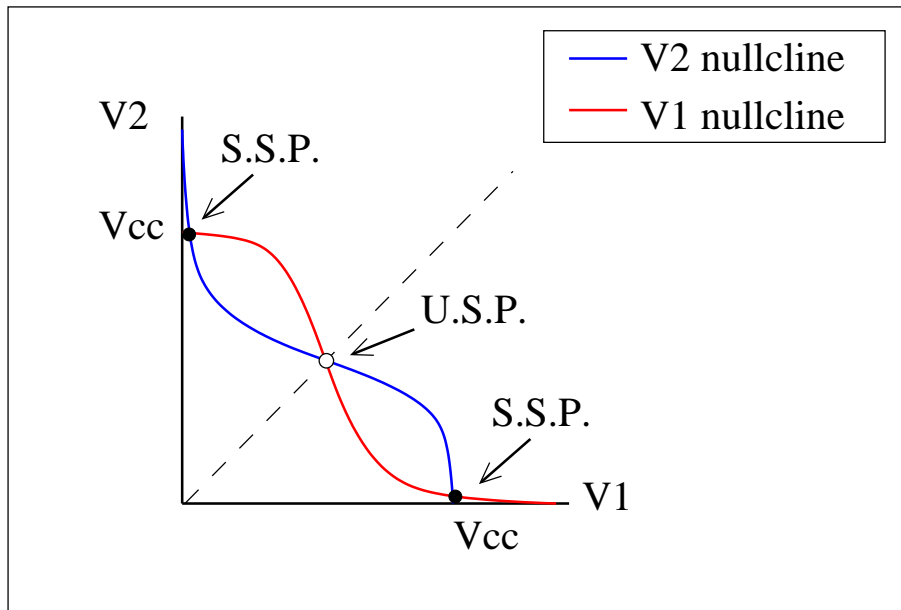


FIG. 10: Phase diagram of the system described in the Eqs. (7) and (8). There are three stationary points in the system: two stable (S.S.P.) and one unstable (U.S.P.). The nullclines are in solid red and blue lines. The separatrix dividing the two basins of attraction is drawn as a dashed line.

transistor T1 (i.e. turn on T2). Next, we turn off T2, leading to a turn-on of T1.

Figure 11 shows the evolution of a population of toggle switches in response to a global external driving. The upper plot depicts the inducing voltage, and the lower plot shows the mean voltage of T1 for the whole population of repressilators. The system, which is initially at the high state, suffers the action of an external inducer at step 4. The output voltage of the population of repressilators decreases until the system jumps towards the off state. At step 8 we stop the inducing action and the system remains off. The turning-on process begins at step 12, where a forcing potential is applied, in this case, at the T2 output. A jump to the high state is observed after step 15, remaining at this point even when the external inducer is removed.

The results obtained with the ETS match with those reported in a real genetic network [5]. The advantage of using ETS is that its simplicity allows to test different configurations of coupling. It can be easily coupled with other circuit like a repressilator so that the study

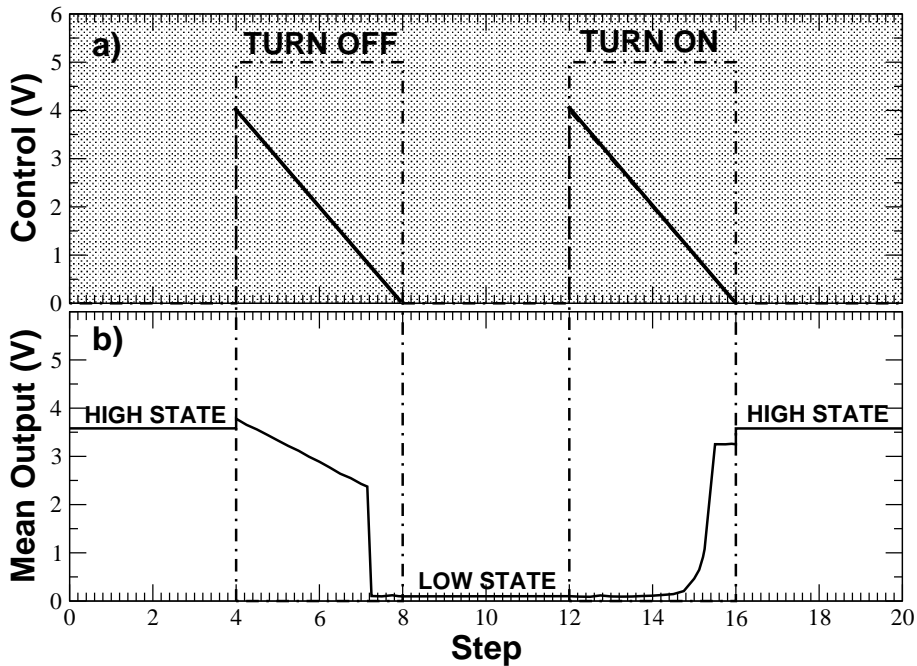


FIG. 11: Control of an electronic toggle-switch population by external forcing. Starting from all bistable switches at the high state, we induce a jump by forcing repressor 1 of each toggle-switch with an external potential (steps 4 to 8). In the absence of forcing the toggle-switch population keeps its state (steps 8 to 12). We can turn on the system again by forcing the opposite repressor (step 12 to 16). The system keeps its state when external forcing is removed (step 16 to 20).

of the dynamics of these complex systems results simple.

VI. CONCLUSIONS

The collective behavior of multicellular populations of synthetic genetic networks is still largely unexplored experimentally, due to difficulties arising from an insufficient characterization of the biochemical elements involved. We have proposed here the use of nonlinear electronic circuits to analyze this problem. **Specifically, we have designed an *electronic repressilator*, constructed under the same operating conditions as the *genetic repressilator*.** Using electronic repressilators, we have analyzed the effect of global coupling in the synchronization of a population of repressilators, observing frequency and phase locking of the whole population. Next, we have studied the influence of an external forcing in the synchronization of the system and we have seen that despite that we obtain frequency locking, phase locking is not achieved. The results indicate that external forcing is a suitable technique to enhance synchronization in combination with coupling between repressilators, but is less efficient when applied by itself. **This conclusion should be taken into account when designing methods to synchronize genetic oscillators.** In addition, we have constructed an electronic toggle switch that behaves in the same way as the corresponding synthetic genetic network. We showed that the dynamics of this population of genetic networks can be reproduced with simple electronic circuits. **It is worth noting that stochastic terms have been neglected here in order to focus on the interplay between coupling and external forcing.** In this sense, further work should address the influence of noise in the synchronization of this kind of systems. Finally, it would be interesting to study different network structures, such as random or small-world networks, by constructing integrated circuits with large numbers of these circuits.

Acknowledgments

Financial support from MCyT (Spain) and FEDER is acknowledged under Projects No. BFM2003-03081 (A.W. and M.A.F.S.) and BFM2003-07850 (J.M.B. and J.G.O.). Partial support to J.M.B. and J.G.O. was also provided by the Generalitat de Catalunya.

-
- [1] F. Jacob and J. Monod, “Genetic regulatory mechanisms in the synthesis of proteins”. *J Mol Biol.* **3**, 318–356 (1961).
- [2] A-L Barabási and Z. N. Oltvai, “Network biology: understanding the cell’s functional organization”, *Nature Rev. Genetics* **5**, 101–113 (2004).
- [3] C. Yanofsky, “Attenuation in the control of expression of bacterial operons”, *Nature* **289**, 751–758 (1981).
- [4] A. Becskei and L. Serrano, “Engineering stability in gene networks by autoregulation”. *Nature* **405**, 590–593 (2000).
- [5] T. S. Gardner, C. R. Cantor, and J. J. Collins, “Construction of a genetic toggle switch in *Escherichia coli*”, *Nature* **403**, 339–342, (2000).
- [6] M.B. Elowitz and S. Leibler, “A synthetic oscillatory network of transcriptional regulators”, *Nature* **403**, 335–338 (2000).
- [7] J. García-Ojalvo, M.B. Elowitz and S. Strogatz, “Modeling a synthetic multicellular clock: Repressilators coupled by quorum sensing”, *Proc. Natl. Acad. Sci. U.S.A.* **101**, 10955–10960 (2004).
- [8] J. Mason, P.S. Linsay, J.J. Collins and L. Glass, “Evolving complex dynamics in electronic models of genetic networks”, *Chaos* **14**, 707–715 (2004).
- [9] D. McMillen, N. Kopell, J. Hasty and J.J. Collins, “Synchronizing genetic relaxation oscillators by intercell signaling”, *Proc. Natl. Acad. Sci. USA* **99**, 679–684 (2002).
- [10] L. You, R.S. Cox, R. Weiss and F.H. Arnold, “Programmed population control by cell-cell communication and regulated killing”, *Nature* **428**, 868–871 (2004).
- [11] Y. Kuramoto, “*Chemical Oscillations, Waves, and Turbulence*”, SpringerVerlag (1984).
- [12] S.H. Strogatz, “From Kuramoto to Crawford: Exploring the onset of synchronization in populations of coupled oscillators”, *Physica D* **143**, 1–20 (2000).
- [13] I. Z. Kiss, Y. Zhai and J. L. Hudson, “Emerging coherence in a population of chemical oscillators”, *Science* **296**, 1676–1678 (2002).
- [14] H. Kori and A. S. Mikhailov, “Entrainment of Randomly Coupled Oscillator Networks by a Pacemaker”, *Phys. Rev. Lett.* **93**, 254101 (2004).
- [15] D. Bell-Pedersen, V. M. Cassone, D. J. Earnest, S. S. Golden, P. E. Hardin, T. L. Thomas, and

- M. J. Zoran, “Circadian rhythms from multiple oscillators: lessons from diverse organisms”, *Nature Rev. Genetics* **6**, 544 (2005).
- [16] M. Menaker, “Circadian photoreception”, *Science* **299**, 213 (2003).
- [17] S. Yamaguchi, H. Isejima, T. Matsuo, R. Okura, K. Yagita, M. Kobayashi, and H. Okamura, “Synchronization of cellular clocks in the suprachiasmatic nucleus”, *Science* **302**, 1408 (2003).
- [18] V. Anishchenko, A. Neiman, A. Astakhov, T. Vadiavasova, and L. Schimansky-Geier, *Chaotic and Stochastic Processes in Dynamic Systems* (Springer Verlag, Berlin, 2002).